# MODELING COMMERCIAL ADAPTIVE CRUISE CONTROL (ACC) ON MULTI- LANE FACILITIES BY INCORPORATING RECEIVING-LANE-CHANGE CAR-FOLLOWING

Mingyuan Yang, Mohamed Badhrudeen, Xingan David Kan, Kemal Yagantekin, Xiao-yun Lu

Abstract— Today's mainstream vehicles are partially automated via an advanced driver assistance system (ADAS) including Adaptive Cruise Control (ACC). ACC uses on-board remote sensor target detection and tracking to automatically adjust speed to maintain a constant time-gap. Contrary to expectations, ACC may reduce capacity at bottlenecks because its delayed response and limited acceleration during queue discharge could increase the average headway. However, this has not been investigated for cases when lane changers enter from the adjacent lane, which prevents accurate analysis for multi-lane roadways. ACC could respond differently for those scenarios, and such car following behavior is often referred as receiving-lane-change (RLC) car following. Using data from carefully planned field tests on lane change car following an RLC car following model was developed in this study. This model has then been integrated into a comprehensive ACC car-following model for microscopic traffic simulation. Lastly, this study proposed a revised ACC car-following model to represent electric vehicles (EV) with ACC, that exhibit significantly different braking and acceleration characteristics verses internal combustion (IC) engine ACC-vehicles.

# I. INTRODUCTION

Advancements in vehicle automation and driver assistance could present new opportunities to improve roadway capacity. While full automation is not yet commercially available, partial automation of different SAE levels has come into practice. Most new production vehicles today are equipped with adaptive cruise control (ACC), which can automatically adjust the vehicle speed to keep a constant time-gap selected by the driver to maintain a safe following distance.

Many researchers have investigated the impact of ACC on traffic flow; recent research has conducted field experiments and developed models that demonstrated that the longitudinal car following behavior of ACC is not string stable [1-7].

M. Yang is with the Civil and Environmental Engineering Department at University of California Berkeley, Berkeley, CA 94720 USA (e-mail: mingyuan yang@berkeley.edu).

- M. Badhrudeen is with the Civil, Environmental, and Geomatics Engineering Department at Florida Atlantic University, Boca Raton, FL 33431 USA (email: mmohamedrawoof@fau.edu).
- X. D. Kan is with the Civil, Environmental, and Geomatics Engineering Department at Florida Atlantic University, Boca Raton, FL 33431 USA (corresponding author, email: kanx@fau.edu, phone: 561-297-3743)
- K. Yagantekin is with the Civil, Environmental, and Geomatics Engineering Department at Florida Atlantic University, Boca Raton, FL 33431 USA (email: kyagantekin2016@fau.edu).
- X. Y. Lu is with Partners for Advanced Transportation Technology (PATH) at University of California Berkeley, Richmond, CA 94804 USA (email: xiaoyun.lu@berkeley.edu).

Moreover, ACC's response to speed fluctuations could lead to an increase in average headway during queue discharge, and this could lead to reduced capacity, as suggested by recent field experiments [8]. To capture this phenomenon, many have constructed microscopic level car following models and macroscopic level models such as the fundamental diagram [9-14]. Furthermore, others have investigated the interaction between ACC and human driver vehicles [15]. However, an important component of ACC car following is missing: how ACC equipped vehicles behave when responding to lane changing (done manually) maneuvers from the adjacent lanes. The car following behavior of the subject vehicle after a lane changing vehicle entered in the immediate front from an adjacent lane, could greatly affect capacity of multilane roadways. This car following behavior is often referred to as RLC car following [16, 17]. In the past, lane change and the subsequent RLC car following behavior of human drivers could reduce capacity at multi-lane freeway bottlenecks, and this has been investigated by various empirical studies [18, 19]. Unfortunately, RLC car following has rarely been addressed in research related to ACC's impact on traffic flow. Some data collection efforts have attempted to integrate RLC car following (also referred as "cut-in") [3]. Another study has recently conducted controlled field tests to isolate the effect of lane changes and investigate the impact of free-flow speed, lane-change speed, and ACC gap setting on RLC car following behaviors [8]. However, there has not been any microscopic RLC car following model that accurately captures the subsequent car following behaviors after lane change occurs, for ACC equipped vehicles.

This study intends to develop microscopic RLC car following models using trajectory data collected from the carefully designed controlled experiments [8] for internal combustion powered vehicles and provide an initial peek at fully electric vehicles.

In the following section, the experimental design and data collection are summarized, followed by the proposed microscopic car following model for RLC. Finally, conclusions and recommendations will be discussed.

# II. OVERVIEW OF FIELD EXPERIMENTS

The experiments were conducted in controlled environments using mainstream ACC equipped vehicles with similar power to weight ratios (internal combustion or IC engine: Toyota Corolla, EV: Hyundai Ioniq 5). As shown in Figure 1a, the front and rear vehicles initially switched to the left lane, then manually accelerated to an initial free-flow

speed of 96 km/hr (60 mph). Then the front vehicle remained at 96 km/hr (60 mph) throughout the experiment. The driver of the rear vehicle activated ACC while maintaining a reasonably short following distance to mimic traffic at or near capacity. Concurrently, middle vehicle remained in the right lane and rapidly accelerated to briefly exceed 96 km/hr (60 mph) drive ahead of both the front and rear vehicles, also illustrated in Figure 1a. Afterwards, the middle vehicle decelerated to 80 km/hr (50 mph) and remained at 80 km/hr (50 mph) until the front and rear vehicles approach from the left lane at 96 km/hr (60 mph). Shown in Figure 1b, once the middle vehicle is aligned with the gap between the front and rear vehicles, the middle vehicle was instructed to manually perform lane change at 80 km/hr (50 mph) and accelerate normally to 96 km/hr (60 mph) during lane change. During the lane change maneuver, we expect ACC in the rear vehicle (follower) to intervene, decelerate to maintain safe following distance and accelerate back to 96 km/hr (60 mph) once the middle vehicle completes the lane change maneuver, as illustrated by Figure 1c and Figure 1d. In addition, the same procedure was repeated with the middle vehicle performing lane changes at 88 km/hr (55 mph) and 96 km/hr (60 mph). Finally, this set of experiments was repeated for initial free-flow speed of 56 km/hr (35 mph) with lane change speeds of 56 km/hr (35 mph), 48 km/hr (30 mph), and 40 km/hr (25 mph). This controlled experiment is intended to replicate disruptive lane change maneuvers into vehicles more closely spaced in the adjacent lane, and these maneuvers typically occur on freeways near its entrances and exits where mandatory lane changes from lower speeds to higher speed traffic are the most common.





(b) Middle vehicle (lane changer in red) decelerates to prepare for lane change



(c) Middle vehicle performs lane change and the ACC in rear vehicle reacts



(d) All three vehicles re-stabilize and return to 60 mph steady state Figure 1. Lane change experiment procedures.

The data and detailed descriptions of the experiment are available in a recent publication on the MicroSIM ACC database [8].

#### III. MODEL DEVELOPMENT

To model the full speed range ACC receiving lane-change car-following behavior, the following PATH model was adopted as the basis of model development [18]:

$$\begin{aligned} a_{sv} &= k_1(v_f - v_{sv}) \\ a_{sv} &= k_2(d - t_{hw}v_{sv} - L) + k_3(v_l - v_{sv}) \end{aligned} \tag{1}$$

where  $a_{sv}$ : acceleration recommended by the ACC controller to the following vehicle  $[m/s^2]$ ;  $k_1$ : gain in positioning difference between the preceding vehicle and the following vehicle;  $k_2$ : gain in speed difference between the preceding vehicle and the following vehicle; d: distance gap between the following vehicle's front bumper and the preceding vehicle's front bumper [m];  $t_{hw}$ : desired time gap of the ACC controller (s); L: length of the preceding vehicle [m];  $v_f$ : the free-flow speed [m/s];  $v_l$ : current speed of the preceding vehicle [m/s];  $v_{sv}$ : current speed of the following vehicle

### A. Proposed New Model Structure for ACC with IC engine.

#### a. Updated Desired Time Gap

A new desired time gap set needs to be adapted to the model, reflecting the latest design of ACC controller embedded in commercial ACC vehicles. The previous time gap was measured from a field test in 2010 [20], which are 31.1% at 2.2 s, 18.5% at 1.6 s; and 50.4% at 1.1 s. To obtain the updated ACC desired time gap, or the ACC minimal safety time gap, separated car-following experiments [8] have been conducted, and the results are shown in Table 2, which indicates that the desired gap varies not only by ACC selected gap setting, but free-flow speed as well. Besides, IC engine vehicle and EV paired with ACC also show some difference in desired time gap, due to EV's responsive regenerative braking that allows for safe operation at shorter gaps or headways. In this study, since the lane-change experiments were conducted at the free-flow speed of 60 mph and 35 mph, only the desired time gap at the corresponding speed level are shown in the table.

Table 1 Minimum safety time gap (s) under different gap settings and free-flow speed.

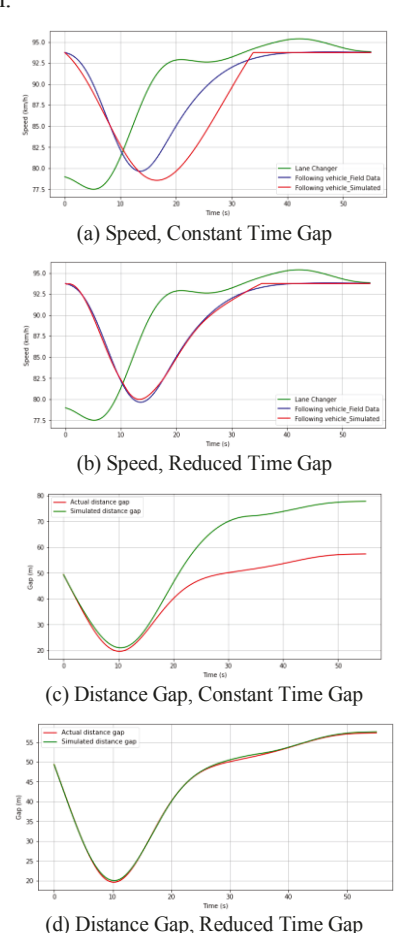
	Desired Time Gap (s)			
Gap Setting	ICE vehicle		EV	
	60 mph	35 mph	60 mph	35 mph
Short	1.18	1.64	1.06	1.14
Medium	1.78	2.47	1.33	1.43
Long	2.16	2.51	1.60	1.66
Extra Long	/		2.13	1.95

## b. Reduced Time Gap

The first major update to PATH model is to develop a time-variant desired time gap  $t_{hw}$  instead of maintaining desired time gap  $t_{hw}$ . Otherwise, the recalibrated model parameters cannot accurately replicate the field observed receiving car following behavior, including the speed profiles and the gap between the following vehicle and the preceding vehicle. The unsatisfactory fit could be attributed to the following vehicle's overestimated deceleration in response to the cut-in maneuver, which leads to the simulated speed lower than the field observed speeds during the deceleration phase. To address this, a reduced time gap  $t_{hw}$  needs to be applied once the cut-in vehicle's lane change maneuver is detected by the ACC controller of the following vehicle.  $t_{hw}$ , s formula is shown as equation 3:

$$\dot{t}_{hw} = t_{min} + (t_{hw} - t_{min}) * \frac{n}{I_s}, n \le I_s$$
 (3)

where  $I_s$  represents the total number of transition time steps, n represents the current time since the detection of the cut-in maneuver,  $t_{min}$  is the minimum temporal time gap the ACC controller will adapt and it should be proportional to be the original desired time gap  $t_{hw}$ . A reasonable search range of this variable is between 0.3-0.7  $t_{hw}$  based on the preliminary examination of the field data. Figure 2 gives a representative example of the simulated speed profile and distance gap with constant desired time gap on the left and time-variant desired time gap on the right, while the free-flow speed is 96 km/hr (60 mph), lane-change speed is 80 km/hr (50 mph), and the gap setting is medium. It proves that applying a reduced time gap is necessary to capture the realistic and less aggressive ACC deceleration in response to the lane change maneuver, keep a relatively higher speed at the beginning of the lane-change, and maintain a shorter distance gap before acceleration.



Simulated speeds and distance gaps with different car-following models (Free-flow speed: 96 km/hr or 60 mph, lane-change speed: 80 km/hr or 50 mph, gap setting: medium).

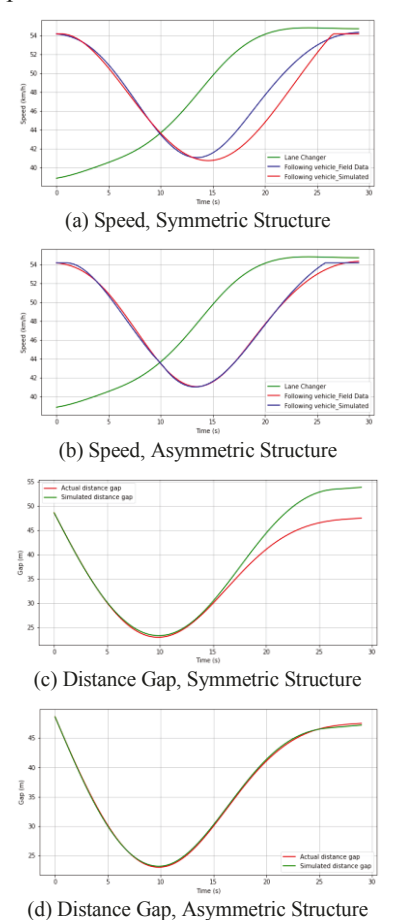
## c. Asymmetric Car-following Behaviors

Another important change to the PATH model is to apply an asymmetric car-following model structure to capture the difference in car following behaviors between acceleration and deceleration stages. The simplest solution is to apply different gap gain  $k_2$  and speed gain  $k_3$  shown in equation 2. Adding the time-variant reduced time gap into consideration, the final receiving lane-change car-following model will be written as equation 4:

$$a_{sv}(t) = \begin{cases} K_{1,1}'(d(t-\tau) - t_{hw}^{\cdot} v_{sv} - L) + K_{2,1}'(v_{lc}(t-\tau) - v_{sv}) \\ if \ a_{sv}(t-1) \le 0 \\ K_{1,2}'(d(t-\tau) - t_{hw}^{\cdot} v_{sv} - L) + K_{2,2}'(v_{lc}(t-\tau) - v_{sv}) \\ if \ a_{sv}(t-1) > 0 \end{cases}$$
Where  $v$  : the lane-change speed  $[m/s]$ 

Where  $v_{lc}$ : the lane-change speed

Figure 3 compares the symmetric and asymmetric model structure in terms of their simulated speed and distance gap, while the free-flow speed is 35 mph, lane-change speed is 25 mph, and the gap setting is long. The figure indicates that the symmetric structure fails to provide enough acceleration strength to let the following vehicle speed up and eventually leads to a longer distance gap than expected after the lane-change process.



Simulated speeds and distance gaps with different car-following models (Free-flow speed: 35 mph, lane-change speed: 25 mph, gap setting:

## d. Smoothing algorithm to transition between acceleration and deceleration.

Further inspection of the field data suggests that the model also requires a smooth transition between acceleration and deceleration to capture the real-world car following behavior. Hence, a simple linear smoothing algorithm was developed and the receiving lane-change car-following model will be rewritten as equation 5:

$$a_{sv}(t) = \begin{cases} a'_{dcc}(t) & a_{sv}(t-1) \le -0.05 \\ a'_{acc}(t) & a_{sv}(t-1) \ge 0.05 \\ a'_{acc}(t) * \frac{a_{sv}(t-1) + 0.05}{0.1} & -0.05 < a_{sv}(t-1) < 0.05 \end{cases}$$
(5)

where  $a'_{dec}(t)$  and  $a'_{acc}(t)$  represents the desired acceleration at time step t if calculated by equation 4 [m/s<sup>2</sup>].

It is worth mentioning that the transition threshold of the acceleration should be selected carefully. On the one hand, the threshold cannot be too large. Otherwise, the model's performance will be greatly affected. On the other hand, the threshold cannot be too small, otherwise the desired acceleration difference could be too large to make the transition happen within the entire threshold. In this study, the threshold is selected as -0.05 - 0.05 m/s<sup>2</sup>.

#### e. Other considerations.

Delay/reaction time  $\tau$  is an important characteristic of the commercial ACC systems as demonstrated in prior field tests [9-12, 16]. Any information obtained from the preceding vehicle should have a time delay before they can be used to estimate the desired acceleration of the following vehicle. In detail, the distance between two vehicles' front bumper  $d(t-\tau)$  applied in the gap regulation term and the preceding vehicle's speed  $v_i(t-\tau)$  applied in the speed regulation term should both add a delay when calibrating the models. In our study, the test vehicles have three different gap settings: short, medium, long. Each gap setting should have its own reaction time. In general, we expect that the larger desired gaps to have longer reaction times.

Besides, we should consider several constraints of the commercial ACC system, including: 1) reasonable thresholds for calibration parameters; 2) physical constraints: maximum acceleration and deceleration limits; 3) speed constraints: speed can never go over the free-flow speed; 4) acceleration constraints: acceleration can never be positive if the leading vehicle is decelerating at congested conditions. These constraints will be added in the final model framework.

B. Final Model Framework Integrated with Regular Car-following Model for IC engine equipped ACC.

To integrate the receiving lane-change car-following model (RCF model) to the comprehensive ACC car-following model framework, we first adopted an enhanced PATH model to capture the ACC regular car-following behaviors under congested condition (CCF model or congested car following model) presented in a previous study [11], listed in equation 6:

$$a_{sv}(t) = \begin{cases} K_{1,1}(d(t-\tau) - t_{hw}v_f - L) + K_{2,1}(v_l(t-\tau) - v_{sv}) \\ if \ a_{sv}(t-1) \le 0 \ and \ \Delta \ V \ge 10 \\ K_{1,2}(d(t-\tau) - t_{hw}v_{sv} - L) + K_{2,2}(v_l(t-\tau) - v_{sv}) \\ if \ a_{sv}(t-1) \le 0 \ and \ \Delta \ V < 10 \\ K_3(v_l(t-\tau) - v_{sv}(t)) \\ if \ a_{sw}(t-1) > 0 \end{cases}$$
where  $\Delta \ V_s$  speed fluctuation magnitude  $[m/c]$ 

This enhanced PATH model is an asymmetric car-following model as well, but with two main differences compared to the RCF model introduced in this study: (1) during the acceleration stage, there is no gap regulation term. This change is to explain the "increased gap" phenomena due to ACC-controller's delay and reaction time when the speed returns to the free-flow speed after speed fluctuation; (2) instead of adapting the reduced time gap to capture the effect of instantaneous gap decrease, this regular car-following model switches from a time-gap regulation to a distance-gap regulation when the speed fluctuation is relatively large, to capture different car-following behaviors under different speeds based on the field observation.

After determining the CCF model structure, we need to decide the boundary to switch between these two models (CCF vs. RCF). Once the cut-in maneuvers take place, one most obvious characteristic is a sudden change in the object/vehicle that the ACC is following. Therefore, we rely on the change of longitudinal distance gap between the following vehicle and the preceding vehicle to choose the model. If the decrease of the longitudinal distance gap within one time step is larger than one vehicle length plus the minimal safety distance gap, then we should apply the RCF model. Otherwise, the CCF model will be used. The boundary distance gap change will be calculated as equation 7:

where  $d_{l}$ : the travelled distance of the leader if it applies a most severe braking to complete stop [m],  $d_{le}$ : the travelled distance of the lane changer in response to leader's braking [m],  $d_{iam}$ : the jam gap [m],  $\tau_r$ : the reaction time of the human driver [s],  $b_{le}$ : the most severe braking that the lane changer wishes to undertake [m/s<sup>2</sup>],  $\hat{b_l}$ : the lane changer's estimate of leading vehicle's most severe braking capabilities [m/s<sup>2</sup>]. Assuming the two vehicle's braking capabilities are the same, then equation 7 can be simplified to equation 8:

$$\Delta d_{min} = v_{lc} * \tau_r - \frac{v_f^2 - v_{lc}^2}{2 * b} + d_{jam} + L \tag{8}$$
 Therefore, the pseudo code of the new ACC car-following

model is presented as follows:

$$\begin{aligned} & \text{If } d(t_0-1)-d(t_0) \leq \Delta d_{min}; \\ & \text{For } t \geq t_0 \text{ and } v_{sv}(t) = v_l(t) = v_f \text{ not holds}; \\ & a_{sv}(t) = \begin{cases} K_{1,1}(d(t-\tau)-t_{hw}v_f-L)+K_{2,1}(v_l(t-\tau)-v_{sv}) & \text{if } a_{sv}(t-1) \leq 0 \text{ and } \Delta V \geq 20 \text{ mph} \\ K_{1,2}(d(t-\tau)-t_{hw}v_{sv}-L)+K_{2,2}(v_l(t-\tau)-v_{sv}) & \text{if } a_{sv}(t-1) \leq 0 \text{ and } \Delta V \geq 20 \text{ mph} \end{cases} \\ & K_{3}(v_l(t-\tau)-t_{sw}v_{sv}-L)+K_{2,2}(v_l(t-\tau)-v_{sv}) & \text{if } a_{sv}(t-1) > 0 \\ & v_{sv}(t) = v_{sv}(t-\Delta t)+a_{sv}(t)\Delta t; \\ & d(t) = d(t-\Delta t)+(v_l(t)-v_{sv}(t))\Delta t; \end{aligned} \\ & \textbf{Else:} \end{aligned}$$

$$\begin{aligned} & \textbf{For } t \geq t_0 \text{ and } v_{sv}(t) = v_l(t) = v_f \text{ not holds}; \\ & k_{1,1}'(d(t-\tau)-t_{hw}v_{sv}-L)+K_{2,1}'(v_{lc}(t-\tau)-v_{sv}) & \text{if } a_{sv}(t-1) \leq 0 \\ & K_{1,2}'(d(t-\tau)-t_{hw}v_{sv}-L)+K_{2,2}'(v_{lc}(t-\tau)-v_{sv}) & \text{if } a_{sv}(t-1) > 0 \end{cases} \\ & v_{sv}(t) = v_{sv}(t-\Delta t)+a_{sv}(t)\Delta t; \\ & d(t) = d(t-\Delta t)+(v_{lc}(t)-v_{sv}(t)\Delta t; \\ & d(t) = d(t-\Delta t)+(v_{lc}(t)-v_{sv}(t)\Delta t; \\ & k_{hw} = t_{min}+(t_{hw}-t_{min})*\frac{t-t_0}{l_s}, t \leq t_0+l_s; \\ & t_{hw} = t_{hw}, t > t_0+l_s; \end{aligned}$$

$$\begin{aligned} & W \text{here:} \end{aligned}$$

Figure 4. Pseudo Code of Congested Car Following Model (CCF) and RLC Car Following Model (RCF) Integration.

After solving a simple linear optimization problem, examples of optimal model parameters of a few cut-in scenarios are shown as follows:

- 35 mph Free-flow speed, 25 mph lane-change speed, long gap setting:  $K_{1\ 1}{}'=0.025$ ,  $K_{2\ 1}{}'=0.135$ ,  $K_{1\ 2}{}'=0.04$ ,  $K_{2\ 2}{}'=0.125$ ,  $I_{\rm s}=8.8$ ,  $t_{min}=0.48\ t_{hw}$ ;
- 60 mph Free-flow speed, 50 mph lane-change speed, medium gap setting:  $K_{1\,1}{}'=0.021$  ,  $K_{2\,1}{}'=0.155$  ,  $K_{1\,2}{}'=0.03$  ,  $K_{2\,2}{}'=0.215$  ,  $I_s=17, t_{min}=0.31\,t_{hw}$ ;
- 60 mph Free-flow speed, 60 mph lane-change speed, short gap setting:  $K_{1\ 1}{}'=0.0245$ ,  $K_{2\ 1}{}'=0.225$ ,  $K_{1\ 2}{}'=0.042$ ,  $K_{2\ 2}{}'=0.225$ ,  $I_{\rm s}=11$ ,  $t_{min}=0.48\ t_{hw}$ .

The threshold for each constraint is determined based on field observations and some simple simulation trials of the collected data. The comprehensive ACC car-following model framework will be briefly represented as the flow chart shown in Figure 5.

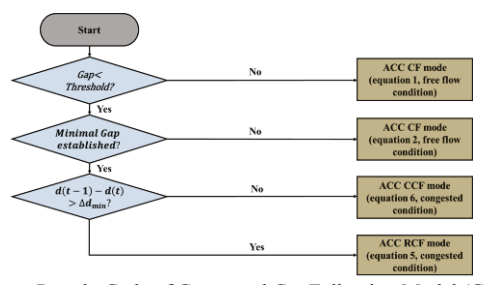


Figure 5. Pseudo Code of Congested Car Following Model (CCF) and RLC Car Following Model (RCF) Integration.

### C. Potential Changes to EVs.

As for RLC car following model, more detailed investigation is required but similar model framework will be applied for EV with ACC as they still have apparent asymmetric car following behaviors. Figure 12 and Figure 13 are examples of how the new RCF model can fit the EV cut-in scenario. The setup is the same as that for IC engine. Some example calibration parameters include the following:

- 60 mph Free-flow speed, 50 mph lane-change speed, medium gap setting:  $K_{1\,1}{}'=0.06$ ,  $K_{2\,1}{}'=0.45$ ,  $K_{1\,2}{}'=0.045$ ,  $K_{2\,2}{}'=0.18$ ,  $I_{\rm s}=3$ ,  $t_{min}=0.82*t_{hw}$  (Figure 6);
- 60 mph Free-flow speed, 60 mph lane-change speed, short gap setting:  $K_{11}' = 0.10$ ,  $K_{21}' = 0.145$ ,  $K_{12}' = 0.025$ ,  $K_{22}' = 0.145$ ,  $I_s = 3.6$ ,

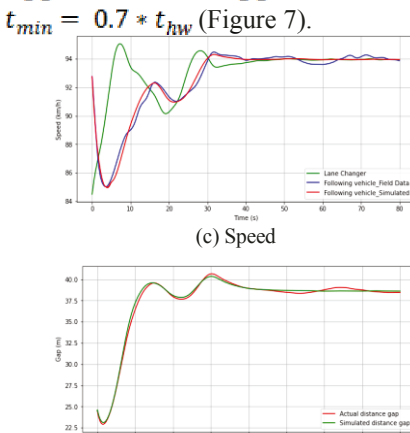


Figure 6. Simulated speeds and distance gap with adjusted RCF model for EV (Free-flow speed: 60 mph, lane-change speed: 50 mph, gap setting: medium)

(d) Distance Gap

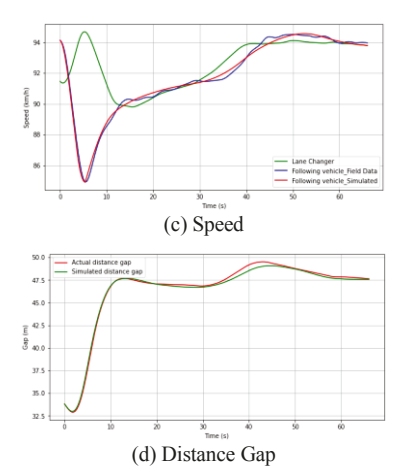


Figure 7. Simulated speeds and distance gaps with adjusted RCF model for EV (Free-flow speed: 60 mph, lane-change speed: 60 mph, gap setting: short).

The preliminary results are consistent with our expectation that greater gain in speed difference and position difference, larger reduced minimum gap and shorter transition time will occur compared to those for IC engine under the same condition. Instantaneous torque and regenerative braking characteristics allow EV with ACC to deliver stronger

acceleration and deceleration so that they can respond more quickly and instantaneously to cut-in vehicles and be less dependent on reduced time gap..

## IV. CONCLUSION AND RECOMMENDATIONS

Automated Vehicles (AVs) have been highly anticipated as they promise to potentially reduce congestion. Vehicles equipped with the full-speed range Adaptive Cruise Control (ACC) are now available on mainstream vehicles today. Besides, the increasing adoption of fully electric vehicles (EVs) has brought new research interests as EV's unique operating characteristics such as instantaneous torque and strong regenerative braking could improve capacity and mitigate congestion when EVs are paired with ACC. Therefore, understanding car following behaviors of both IC engine vehicles and EVs paired with ACC becomes crucial to modeling traffic flow at the microscopic level. One missing component of ACC car following car following in response to lane changes from the adjacent lanes. Without it, the analysis cannot be done for multilane facilities.

Using data from a controlled experiment, a new ACC car-following model has been proposed to better capture the RLC car following behaviors. The new model successfully captures the initial minimum safety gap relaxation adopted by the ACC controller by adopting the reduced time gap and an asymmetric structure. Additional refinement includes incorporating delayed reaction of ACC controller and considering vehicle's physical constraints such acceleration limits. The model was then integrated into a comprehensive ACC car-following framework with multiple boundary conditions, which covers a wide range of real-world traffic scenarios. This framework included other models introduced in previous studies [11, 16, 20]. Lastly, the difference between IC engine and EV in terms of their ACC RLC car following behaviors has been briefly discussed, and potential modified suggestions for EV RCF model has been proposed to capture the more responsive braking and acceleration in receiving car following. The results are consistent with our expectation that EV paired with ACC has a great potential to reverse the negative impact of ACC controller by recovering the gap more instantaneously, and thus relieve the traffic congestion and increase the road capacity.

We recommend future work to apply the proposed ACC car-following model framework in microscopic simulation for prospective evaluation of ACC impact (on both IC engine power vehicles and EVs) to traffic capacity. Furthermore, the proposed model will serve as an important tool for developing macroscopic models such as the fundamental diagram and control strategies for mixed traffic conditions with human driven vehicles and ACC-equipped vehicles with distinct powertrains.

#### REFERENCES

- [1] Ciuffo, Biagio, et al. "Requiem on the positive effects of commercial adaptive cruise control on motorway traffic and recommendations for future automated driving systems." *Transportation Research Part C: Emerging Technologies* 130 (2021): 103305.
- [2] Li, Tienan, et al. "Car-following behavior characteristics of adaptive cruise control vehicles based on empirical experiments." *Transportation Research Part B: Methodological* 147 (2021): 67–91.
- [3] Makridis, Michail, et al. "OpenACC. An open database of car-following experiments to study the properties of commercial ACC systems." *Transportation Research Part C: Emerging Technologies* 125 (2021): 103047.
- [4] Gunter, George, et al. "Are commercially implemented adaptive cruise control systems string stable?." *IEEE Transactions on Intelligent Transportation Systems* 22.11 (2020): 6992-7003.
- [5] Makridis, Michail, et al. "Empirical study on the properties of adaptive cruise control systems and their impact on traffic flow and string stability." *Transportation Research Record* 2674.4 (2020): 471-484.
- [6] Gunter, George, et al. "Model-based string stability of adaptive cruise control systems using field data." *IEEE Transactions on Intelligent* Vehicles 5.1 (2019): 90-99.
- [7] Knoop, Victor L., et al. "Platoon of SAE level-2 automated vehicles on public roads: Setup, traffic interactions, and stability." *Transportation Research Record* 2673.9 (2019): 311–322.
- [8] Yang, Mingyuan, et al. " MicroSimACC: An Open Database for Field Experiments on the Potential Capacity Impact of Commercial Adaptive Cruise Control (ACC)." *Transportmetrica A: Transport Science* (2024): accepted.
- [9] He, Yinglong, et al. "Physics-augmented models to simulate commercial adaptive cruise control (ACC) systems." *Transportation Research Part C: Emerging Technologies* 139 (2022):103692.
- [10] Shang, Mingfeng, Benjamin Rosenblad, and Raphael Stern. "A novel asymmetric car following model for driver assist enabled vehicle dynamics." *IEEE Transactions on Intelligent Transportation Systems*. 23.9 (2022): 15696-15706.
- [11] Yang, Mingyuan, et al. Modeling CAV car following on freeways and arterials – case study of adaptive cruise control (ACC) equipped vehicles. TRBAM-22-02452. 2022.
- [12] Yang, Mingyuan, Xingan David Kan, and Kemal Yagantekin. Modeling Car Following Behaviors of Adaptive Cruise Control (ACC) Equipped Vehicles under Heterogeneous Desired Speeds. TRBAM-23-04056, 2023.
- [13] Shi, Xiaowei, and Xiaopeng Li. "Empirical study on car-following characteristics of commercial automated vehicles with different headway settings." *Transportation Research Part C: Emerging Technologies* 128 (2021): 103134
- [14] Milanés, Vicente, and Steven E. Shladover. "Modeling cooperative and autonomous adaptive cruise control dynamic responses using experimental data." *Transportation Research Part C: Emerging Technologies* 48 (2014): 285-300.
- [15] Gong, Yaobang, et al. Field experiment of mixed traffic interaction between adaptive cruise control (ACC) and human drivers. TRBAM-22-03779. 2022.
- [16] Kan, Xingan David, et al. "Cross-comparison and calibration of two microscopic traffic simulation models for complex freeway corridors with dedicated lanes." *Journal of Advanced Transportation* 2019 (2019): 8618476.
- [17] Liu, Hao, et al. "Modeling impacts of cooperative adaptive cruise control on mixed traffic flow in multi-lane freeway facilities." *Transportation Research Part C: Emerging Technologies* 95 (2018): 261-279.
- [18] Cassidy, Michael J. and Jittichai Rudjanakanoknad "Increasing the capacity of an isolated merge by metering its on-ramp." *Transportation Research Part B: methodological* 39.10 (2005): 896–913.
- [19] Cassidy, Michael J. and Robert Bertini "Some traffic features at freeway bottlenecks." *Transportation Research Part B: Methodological* 33.1 (1999): 25–42.
- [20] Novakowski, Christopher, et al. "Cooperative adaptive cruise control: Driver acceptance of following gap settings less than one second." Human Factors and Ergonomics Society Annual Meeting 54.24 (2010): 2033-2037